Discovery of the novel mTOR inhibitor and its antitumor activities *in vitro* and *in vivo*

Hua Xie[1,2], Mee-Hyun Lee[1], Feng Zhu[1], Kanamata Reddy[1], Zunnan Huang[1], Dong Joon Kim[1], Yan Li[1], Cong Peng[1], Do Young Lim[1], Soouk Kang[1], Sung Keun Jung[1], Xiang Li[1], Haitao Li[1], Weiya Ma[1], Ronald A. Lubet[3], Jian Ding[2], Ann M. Bode[1], Zigang Dong[1]

Notes: H. Xie, MH. Lee and F. Zhu contributed equally to this work.

Author Affiliations:

[1] The Hormel Institute, University of Minnesota, Austin, Minnesota, USA

[2] State Key Laboratory of Drug Research, Shanghai Institute of Materia Medica, Chinese Academy of Sciences, Shanghai, China

[3] National Institutes of Health, National Cancer Institute, MD, USA

Running Title: Discovery of mTOR inhibitor 3HOI-BA-01 antitumor activities

Keywords: mammalian target of rapamycin, anti-tumor activity, lung cancer, cell signal transduction, anchorage-independent growth

Correspondence: Zigang Dong, The Hormel Institute, University of Minnesota, 801 16th Avenue NE, Austin, MN 55912-3679. Phone: 507-437-9600; Fax: 507-437-9606; Email: zgdong@hi.umn.edu

Word count: 4349

Total number of figures: 6 Figures

1

Disclosure of Potential Conflicts of Interest: The authors declare no potential conflicts of interest.

2

Abstract

The phosphatidylinositol 3-kinase (PI3-K)/Akt and mammalian target of rapamycin (mTOR) signaling pathway plays a critical role in cell survival and proliferation and is often aberrantly activated in many types of cancer. The mTOR kinase protein, one of the key molecules in this pathway, has been shown to be an important target for cancer therapy. In the present study, a ligand docking method was used to screen for novel scaffold mTOR inhibitors. Sixty thousand compounds in the Natural Product Database (NPD) were screened against the mTOR homologous structure and 13 commercially available compounds listed in the top-ranked 100 compounds were selected for further examination. Compound (*E*)-3-(4-(benzo[*d*][1,3]dioxol-5-yl)-2-oxobut-3-en-1-yl)-3-hydroxyindolin-2-one; designated herein as 3HOI-BA-01) was then selected for further study of its antitumor activity. An *in vitro* study demonstrated that 3HOI-BA-01 inhibited mTOR kinase activity in a dose-dependent manner by directly binding with mTOR. In a panel of NSCLC cells, the compound also attenuated mTOR downstream signaling, including the phosphorylation of p70S6K, S6, and Akt, resulting in G1 cell cycle arrest and growth inhibition. Results of an *in vivo* study demonstrated that i.p. injection of 3HOI-BA-01 in A549 lung tumor-bearing mice effectively suppressed cancer growth without affecting the body weight of the mice. The expression of downstream signaling molecules in the mTOR pathway in tumor tissues was also reduced after 3HOI-BA-01 treatment. Taken together, we identified 3HOI-BA-01 as a novel and effective mTOR inhibitor.

3

Introduction

The phosphatidylinositol 3-kinase (PI3-K)/Akt/ mammalian target of rapamycin (mTOR)

pathway is a signal transduction cascade that is central to a variety of important physiological

functions, including cell survival, protein synthesis and growth, cell cycle, metabolism and

angiogenesis (1-2). PI3-K is activated upon growth factors binding to their cognate receptors,

resulting in the activation of PI3-K-dependent kinases, which then phosphorylate and activate Akt (3).

Phosphorylation of Akt at both serine 473 and threonine 308 is required for its full activation (4). Akt

then activates mTOR by direct phosphorylation and inhibition of tuberous sclerosis complex 2

(TSC2), which is a negative regulator of mTOR. In cells, mTOR exists in at least two functionally

distinct protein complexes, mTORC1 and mTORC2. mTORC1 phosphorylates the p70S6 kinase

(p70S6K), which in turn phosphorylates the S6 ribosomal protein and 4E-BP1, leading to protein

translation (5). mTORC2 functions in a feedback loop to activate Akt by phosphorylation on serine

473 (6).

The PI3K/Akt/mTOR signal transduction pathway is frequently deregulated in human cancers

and thereby has attracted considerable attention as an oncology drug discovery target (7-8). The most

well-characterized inhibitor targeting this pathway is rapamycin and its analogues (also referred as

rapalogs), which are currently used with success for treating several types of tumors (9). Previous

studies have shown that the rapalogs are allosteric inhibitors that, in complex with FKBP12, target

the FKB domain of mTOR (10). They partially inhibit mTOR through allosteric binding to mTORC1,

but not mTORC2 (11). However, inhibiting only mTORC1 may not be sufficient for achieving a

broad and robust anticancer effect due to the failure to inhibit mTORC2 in some tumor types.

Moreover, resistance to treatment with rapamycin/rapalogs has been reported. The resistance has

4

been ascribed, at least in part, to a feedback loop triggered by rapamycin, which leads to activation of Akt through inhibition of p70S6K, thereby, counteracting the antitumor potential of mTOR inhibition (12-13). Therefore, great interest exists in the development of novel mTOR kinase inhibitors, which might suppress both mTORC1 and 2 or might inhibit both mTOR and PI3-K activities, thereby attenuating Akt activation.

In the present study, we identified a novel mTOR inhibitor from the Natural Product Database (NPD) database. The homologous structure of mTOR was used for virtual database screening, and (*E*)-3-(4-(benzo[*d*][1,3]dioxol-5-yl)-2- oxobut-3-en-1-yl)-3-hydroxyindolin-2-one; designated herein as 3HOI-BA-01), was shown to be most effective, possessing *in vitro* and *in vivo* antitumor activity mediated through attenuation of mTOR signaling.

Materials and Methods

Computational modeling

The three-dimensional (3-D) structure of mTOR was obtained from the SWISS-MODEL Repository, which is a kind of homology model based on the crystal structure of PI3-K-delta (PDB id 2WXG). Protein-ligand docking was performed using Glide, which is a high performance hierarchical docking algorithm (14). The final binding model structure of mTOR-3HOI-BA-01 was generated from Schrodinger Induced Fit Docking (15), which merges the predictive power of Prime with the docking and scoring capabilities of Glide for accommodating the possible protein conformational changes upon ligand binding.

Reagents

5

3HOI-BA-01 was purchased from ChemBridge (San Diego, CA) or synthesized in house as previously described (16). The structure of the synthesized molecule was confirmed by ^{1}H NMR and compared with the authentic commercial sample. Rapamycin was purchased from LC Laboratories (Woburn, MA). Recombinant active kinases, mTOR (1362-end), PI3-K and Akt, were purchased from Millipore (Billerica, MA). The inactive p70S6K protein was from SignalChem (Richmond, BC, Canada) and Epoxy-activated Sepharose 6B was purchased from GE Healthcare (Pittsburgh, PA). phosphorylated p70S6K (T389), p70S6K, phosphorylated mTOR (S2448), mTOR, phosphorylated S6 (S235, 236), S6, phosphorylated Akt (S473) and Akt were purchased from Cell Signaling Technology (Beverly, MA). The antibody against β-actin was purchased from Santa Cruz Biotechnology (Santa Cruz, CA).

Cell culture

NSCLC cell lines, A549, H520, H1650, and the mouse epidermal cell line, JB6 Cl41, were purchased from American Type Culture Collection (ATCC, Manassas, VA). A549 cells were cultured in F-12K containing penicillin (100 units/mL), streptomycin (100 µg/mL), L-glutamine (2 mM), and 10% FBS (Life Technologies, Grand Island, NY). H520 cells and H1650 cells were cultured in RPMI-1640 containing penicillin (100 units/mL), streptomycin (100 µg/mL), L-glutamine (2.05 mM), and 10% FBS (Life Technologies). JB6 Cl41 cells were cultured in Eagle's MEM containing penicillin (100 units/mL), streptomycin (100 µg/mL), and 5% FBS. Cells were maintained at 5% CO_2 and 37°C in a humidified incubator. Cells were cytogenetically tested and authenticated before the cells were frozen. Each vial of frozen cells was thawed and maintained for about two months (10 passages).

6

Anchorage-independent cell transformation assay

NSCLC cell lines were suspended in Basal Medium Eagle (BME) medium and added to 0.6%

agar, with vehicle or 5, 10, 20 µM 3HOI-BA-01 in base and top layers of 0.3 % agar. For JB6 Cl41

cells, the procedure is similar, except that these cells were exposed to EGF (20 ng/mL) during

treatment with 3HOI-BA-01 or vehicle. The cultures were maintained at 37°C in a 5% CO_2 incubator

for 1 to 2 weeks and then colonies were counted under a microscope using the Image-Pro Plus

software (v6.1) program (Media Cybernetics, Silver Spring, MD).

Cell cycle analysis

A549 cells were seeded on 60-mm plates and treated or not treated with 3HOI-BA-01 for 72 h.

Then cells were fixed in 70% ethanol and stored at -20 °C overnight. Propidium iodine staining of

DNA was performed to determine cell cycle distribution using a BD FACSCalibur Flow Cytometer

(BD Biosciences, San Jose, CA).

MTS assay

To estimate cytotoxicity, JB6 Cl41 cells were seeded (8×10^3 cells per well) in 96-well plates and

cultured overnight. Cells were then fed with fresh medium and treated with vehicle or 5, 10, 20, 40,

or 80 µM 3HOI-BA-01. After culturing for 24 or 48 h, the cytotoxicity of 3HOI-BA-01 was

measured using an MTS assay kit (Promega, Madison, WI) according to the manufacturer's

instructions.

Western blot analysis

7

Western blotting was performed as previously reported (17). In brief, proteins were resolved by SDS-PAGE and transferred onto polyvinylidene difluoride membranes (Millipore, MA), which were blocked with nonfat milk and hybridized with specific primary antibodies. The protein bands were visualized using an enhanced chemiluminescence reagent (GE Healthcare, Pittsburgh, PA) after hybridization with a horseradish peroxidase-conjugated secondary antibody.

mTOR *in vitro* kinase assay

Inactive S6K proteins (1 μg) were used as the substrate for an *in vitro* kinase assay with 250 ng of active mTOR (1362-end). Reactions were carried out in 1 × kinase buffer (25 mM Tris-HCl pH 7.5, 5 mM beta-glycerophosphate, 2 mM dithiothreitol (DTT), 0.1 mM Na_3VO_4, 10 mM $MgCl_2$ and 5 mM $MnCl_2$) containing 100 μM ATP at 30°C for 30 min. Reactions were stopped and proteins detected by Western blotting.

PI3-K *in vitro* kinase assay

The PI3-K *in vitro* kinase assay was performed as previously described (18). Briefly, 100 ng active PI3-K (Millipore) was incubated with dimethyl sulfoxide (DMSO) or 3HOI-BA-01 for 15 min and then reacted with phosphatidylinositol sodium salt (MP Biomedical, Solon, OH). Reactions were performed in kinase buffer containing 50 μM unlabeled ATP with or without 10 μCi of $[\gamma^{-32}P]$ ATP at 30°C for 20 min. Reactions were terminated and resolved by thin layer chromatography (Merck, Whitehouse Station, NJ) and visualized by autoradiography.

Akt1 and Akt2 *in vitro* kinase assays

8

In vitro Akt1 and 2 kinase assays were performed in accordance with the manufacturer's instructions. In brief, an active Akt1 or Akt2 protein (30 ng) and substrate (30 µM) were incubated with or without 3HOI-BA-01 for 30 min at 30°C. Afterward, 20 µl aliquots were transferred onto p81 paper and washed 3 times with 0.75% phosphoric acid for 5 min per wash and once with acetone for 5 min. Radioactive incorporation was determined using a scintillation counter (LS6500; Beckman Coulter, Brea, CA).

In vitro pull-down assay

Recombinant human mTOR (1362-end; 200 ng) or cell lysates (1 mg) were incubated with 3HOI-BA-01-Sepharose 6B beads (or Sepharose 6B beads alone as a control; 100 µL, 50% slurry) in the reaction buffer [50 mM Tris (pH 7.5), 5 mM EDTA, 150 mM NaCl, 1 mM DTT, 0.01% Nonidet P-40, 2 µg/mL bovine serum albumin, 0.02 mM phenylmethylsulfonyl fluoride (PMSF), and 1 µg/mL protease inhibitor mixture]. After incubation with gentle rocking overnight at 4°C, the beads were washed 5 times and proteins bound to the beads were analyzed by Western blotting.

Xenograft mouse model

Athymic nude mice [Cr:NIH (S), NIH Swiss nude, female, 6-week old] were obtained from Harlan Laboratories (Minneapolis, MN) and maintained under "specific pathogen-free" conditions based on the guidelines established by the University of Minnesota Institutional Animal Care and Use Committee. Mice were divided into different groups (n = 8 of each group). A549 lung cancer cells (3×10^6/0.2 mL 1X PBS) were injected subcutaneously into the right flank of each mouse. 3HOI-BA-01 was prepared once a week and protected from light and kept at 4°C. 3HOI-BA-01 or

9

vehicle control was administered by i.p. injection 3 times a week. Tumor volumes were measured 3 times a week and the body weights were measured once a week. Mice were monitored until tumors reached 1-cm^3 total volume, at which time mice were euthanized and tumors extracted and were analyzed by Western blotting.

Statistical analysis

All quantitative data are expressed as means ± S.D. and significant differences were determined by the Student's t test or one-way ANOVA. A probability value of $p < 0.05$ was used as the criterion for statistical significance.

Results

Molecular docking identified 3HOI-BA-01 as a potential mTOR inhibitor

With the purpose of identifying novel inhibitors of mTOR kinase activity, we performed an intensive molecular docking analysis using Glide v5.7 (14) to screen sixty thousand compounds from the Natural Products Database (NPD) against the structure of the homology model of mTOR, which was based on the crystal structure of PI3-K-delta (PDB id 2WXG) (19). The top-ranked 100 compounds were re-docked into mTOR with the Induced Fit Docking (IFD) (15) protocol implemented in Schrodinger Suite 2011. Finally, 13 commercially available compounds were selected from the top-ranked list of 100 and were tested experimentally. 3HOI-BA-01 (Fig. 1A) dramatically inhibited neoplastic cell transformation (data not shown) and was selected for further study. According to the docking result (Fig. 1B), 3HOI-BA-01 formed four hydrogen bonds with the mTOR protein. One hydrogen bond involved the backbone atoms of the hinge residue Val2240 and

10

the other three hydrogen bond were formed with the side chain atoms of Lys2187, Tyr2225 and

Asp2357, respectively. In addition, one phenyl ring formed strong π-π stacking interactions with the

hydroxyphenyl ring of Tyr2225. These results indicate that 3HOI-BA-01 might inhibit mTOR by

directly binding with that protein.

3HOI-BA-01 is a potent inhibitor of mTOR

In order to determine whether 3HOI-BA-01 inhibits mTOR kinase activity, we first

performed an *in vitro* kinase assay with recombinant mTOR in the presence of various concentrations

of 3HOI-BA-01. Wortmannin, a well-known inhibitor of both PI3-K and mTOR, was used as a

positive control in this assay. The phosphorylation of p70S6K (Thr389), an mTOR substrate, was

strongly suppressed by 3HOI-BA-01 in a concentration-dependent manner. A very low concentration

of 3HOI-BA-01 (1 µM; Fig. 2A) caused a 21% inhibition of mTOR kinase activity and 3HOI-BA-01

at 5 µM caused a 67 % inhibition and the highest concentration (20 µM) of 3HOI-BA-01 resulted in

a 95% inhibition. These results clearly indicate that 3HOI-BA-01 is an inhibitor of mTOR kinase

activity.

3HOI-BA-01 binds directly to mTOR

The docking results indicated that 3HOI-BA-01 formed a good interaction with the mTOR

active site, which might be the basis of the direct binding of 3HOI-BA-01 to mTOR, resulting in the

inhibition of mTOR kinase activity. To confirm this idea, we performed an *in vitro* binding assay

using 3HOI-BA-01-conjugated Sepharose 6B beads or control Sepharose 6B beads. No obvious band

was observed when the mTOR protein was incubated with Sepharose 6B beads, whereas a clear band

11

was seen when mTOR was incubated with 3HOI-BA-01-conjugated Sepharose 6B beads (Fig. 2B),

indicating that 3HOI-BA-01 directly binds to recombinant mTOR *in vitro*. We then performed an *ex*

vivo pull-down assay in A549 human lung cancer cells, and similar results were also obtained with

an A549 cell lysate (Fig. 2C). These results indicated that 3HOI-BA-01 binds directly to mTOR

protein and thus inhibits mTOR kinase activity.

3HOI-BA-01 inhibits EGF-induced neoplastic transformation and signal transduction in JB6

Cl41 cells

We then examined the effect of 3HOI-BA-01 on EGF-induced neoplastic transformation of

JB6 Cl41 cells. 3HOI-BA-01 significantly inhibited EGF-promoted neoplastic transformation in a

dose-dependent manner (Fig. 3A). 3HOI-BA-01 at 1, 5, 10, or 20 μM caused a decrease of 18, 19, 62,

or 98% of control, respectively (Fig. 3B). The inhibition of colony formation by 3HOI-BA-01 was

not due to cytotoxicity because the effective concentration range for suppressing cell transformation

did not affect JB6 Cl41 cell viability (Fig. 3C). Because anchorage-independent growth ability is an

ex vivo indicator and a key characteristic of the transformed cell phenotype (20), these results suggest

that 3HOI-BA-01 can reduce the malignant potential of JB6 Cl41 cells induced by EGF.

In order to test whether 3HOI-BA-01 exerts its activity by inhibiting mTOR activity in JB6 Cl41

cell, we treated cells with 3HOI-BA-01 and examined several key signaling molecules, including

those in the RAS/RAF/MEK and PI3-K/Akt/mTOR pathways, which are frequently deregulated in

human malignancies. Western blot results showed that 3HOI-BA-01 dose-dependently suppressed

the phosphorylation of p70S6K and S6 ribosomal protein (S6), which are downstream signaling

molecules of mTOR (Fig. 3D). However, 3HOI-BA-01 had no effect on the phosphorylation of other

12

molecules, including EGFR, RAF, MEK and ERKs (data not shown). This result suggested that the

mTOR signaling pathway accounts for the inhibition of cell transformation by 3HOI-BA-01.

3HOI-BA-01 inhibits downstream targets of both mTORC1 and mTORC2 and suppresses

growth of human lung cancer cells

Previous studies suggested that the mTOR signaling pathway is highly activated in human

lung cancer (21-23). Therefore, we examined the effect of 3HOI-BA-01 in a panel of non-small cell

lung cancer (NSCLC) cells. First, we investigated the effects of 3HOI-BA-01 on

anchorage-independent cell growth and the results showed that 3HOI-BA-01 significantly inhibited

A549 cell growth in soft agar in a concentration-dependent manner (Fig. 4A). Colony formation was

inhibited by more than 50% after treatment with 3HOI-BA-01 at a concentration of 10 µM, and

almost no colonies were formed at 20 µM (Fig. 4A). Moreover, we also examined the effect of

3HOI-BA-01 on the growth of several other lung cancer cell lines, including H520 and H1650.

Results showed that 3HOI-BA-01 dose-dependently inhibited the growth of each cell line in soft agar

(Fig. 4B, C).

We then investigated the effect of 3HOI-BA-01 on downstream targets of mTOR in A549

cancer cells. Western blot results showed that mTORC1-mediated phosphorylation of p70S6K

(T389) and S6 (S235, 236) was substantially decreased dose-dependently with 3HOI-BA-01

treatment (Fig. 4D). Meanwhile, mTORC2-mediated phosphorylation of Akt (S473) was also

inhibited in a dose-dependent manner (Fig. 4D). Moreover, results also showed that the

phosphorylation of mTOR (S2448) was attenuated at the higher concentration (20 µM) of

3HOI-BA-01 (Fig. 4D).

13

Inhibition of mTOR can result in many effects on cells, including cell cycle arrest and apoptosis. Therefore, we examined whether 3HOI-BA-01 affects cell cycle progression and apoptosis. Results revealed that 3HOI-BA-01 treatment led to G1 cell cycle arrest (Fig. 4E). However, no change was observed in sub-G1 population after treatment with 3HOI-BA-01 (data not shown), indicating that it has no effect on apoptosis. These results indicated that, as an mTOR inhibitor, 3HOI-BA-01 could induce cell cycle arrest without affecting apoptosis, which is quite similar to the effects of other reported mTOR inhibitors (24).

3HOI-BA-01 inhibits PI3-K activity at a higher concentration

The inhibition of Akt (S473) and mTOR (S2448) could result not only from mTORC2 inhibition, but also from inhibition of upstream PI3-K or Akt. Thus, we further examined the effects of 3HOI-BA-01 on PI3-K or Akt *in vitro* kinase activity. Class IA PI3-Ks, consisting of PI3-K-α, PI3-K-β and PI3-K-δ, are reportedly implicated in human cancer (25-27). Our results showed that 3HOI-BA-01 suppressed PI3-K-α, PI3-K-β and PI3-K-δ *in vitro* activity in a concentration-dependent manner (Fig. 5A). However, the concentration (10 or 20 μM) that inhibits PI3-K is higher than that required for mTOR inhibition. In addition, we examined the activity of 3HOI-BA-01 in Akt1 and Akt2 *in vitro* kinase assays. Only 30% or less inhibition was observed even at 20 μM 3HOI-BA-01 (Fig. 5B), indicating that Akt1 and Akt2 might not be major targets of 3HOI-BA-01. These results demonstrated that 3HOI-BA-01 targets both mTOR and PI3-K, with PI3-K being much less sensitive.

3HOI-BA-01 inhibits growth of lung cancer cells in a xenograft model

14

To explore the antitumor activity of 3HOI-BA-01 *in vivo*, A549 cancer cells were innoculated into the right flank of individual athymic nude mice. Mice were then administered vehicle or 3HOI-BA-01 (10 or 40 mg/kg body weight, i.e. B.W.) by i.p. injection, 3 times a week for 29 days. The results showed that treatment of mice with 10 or 40 mg/kg B.W. of 3HOI-BA-01 significantly suppressed A549 tumor growth by 58% and 76%, respectively, relative to the vehicle-treated group (Fig. 6A, $p < 0.01$). Moreover, mice seemed to tolerate treatment with these doses of 3HOI-BA-01 without the loss of body weight compared with vehicle-treated group (Fig. 6B). The effect of 3HOI-BA-01 on mTOR protein targets was evaluated by Western blot analysis after 29 days of treatment. The expression of phosphorylated S6, as well as the phosphorylation of Akt (S473), were markedly decreased after treatment with 3HOI-BA-01 (Fig. 6C). These data indicated that A549 lung tumor development was suppressed by 3HOI-BA-01 through inhibition of the PI3-K/mTOR signaling pathway.

Discussion

The aim of this study was to identify novel scaffold inhibitors of mTOR using molecular docking methods. We combined two docking methods, Glide and IFD, for molecular docking in this study. Glide adopts a hierarchical docking algorithm and efficiently improves docking speed (14). However, the protein structure is regarded as a rigid body and protein flexibility is ignored. With IFD, the side chains in the binding pocket are allowed to move so as to simulate the induced fit effect of the protein structure upon ligand binding (15). The disadvantage of IFD is the high computational cost and low speed. To trade off accuracy and speed, Glide was used for the initial screening and IFD was used for refinement of top-ranked compounds. Based on these two methods, sixty thousand

15

compounds in the NPD were screened against the mTOR homologous structure and several

compounds were identified as potential mTOR inhibitors. 3HOI-BA-01, a compound belonging to

the 3-hydroxy-2-oxindole group of compounds, was confirmed to inhibit mTOR kinase activity and

exert antitumor activity.

We first examined the inhibitory activity of 3HOI-BA-01 using an *in vitro* mTOR kinase assay.

3HOI-BA-01 could potently suppress mTOR activity in a concentration-dependent manner. We

further performed *in vitro* binding and *ex vivo* pull-down assays and confirmed the direct binding

between 3HOI-BA-01 and the mTOR protein. In addition, 3HOI-BA-01 inhibited the

phosphorylation of mTOR downstream molecules in cancer cells, including the mTORC1 substrates

p70S6K (T389) and S6 (S235,236) and the mTORC2 substrate Akt (S473), resulting in the inhibition

of the growth of several types of human lung cancer cells. Moreover, results of an *in vivo* study using

a xenograft mouse model further confirmed that 3HOI-BA-01 suppressed mTOR's protein targets in

tumor tissues resulting in inhibition of tumor growth *in vivo*. Therefore, 3HOI-BA-01 inhibits mTOR

kinase activity both *in vitro* and *in vivo* by directing binding with mTOR, which suppressed tumor

growth.

Intriguingly, 3HOI-BA-01 showed inhibitory activity on the phosphorylation of Akt on S473

both in tumor cells and in the xenograft mouse model tumor tissue, indicating an advantage of this

compound over rapalogs in Akt inhibition. Rapalogs have been reported to increase the

phosphorylation of Akt on S473 in cancer cells and patients treated with these drugs eventually

become refractory partly due to Akt activation (28-29). Previous studies showed that mTORC1, but

not mTORC2, is sensitive to rapamycin. The activation of Akt by rapalogs is mainly due to the

disruption of a negative feedback loop, which is dependent on IGF1R/insulin receptor substrate 1

16

(IRS-1), and involves the S6K-mediated suppression of upstream signaling (28-29). mTORC1 inhibitors abrogate this feedback suppression, thus resulting in Akt activation. In the present study, we demonstrated that 3HOI-BA-01 inhibits the phosphorylation of mTORC1 downstream targets, including p70S6K and S6, and the mTORC2 downstream target, Akt. Moreover, this compound also attenuated PI3-K activity at a higher concentration. Therefore, the inhibition of the phosphorylation of Akt (S473) by 3HOI-BA-01 might be the result of both mTORC2 inhibition and of PI3-K inhibition.

Taken together, using a molecular docking method, we identified 3HOI-BA-01 as a novel mTOR/PI3K dual inhibitor, possessing antitumor activity *in vitro* and *in vivo*. Allosteric inhibitors of mTOR have been reported to increase the phosphorylation of Akt. Thus, 3HOI-BA-01, as an mTOR inhibitor, possesses a potential advantage and deserves further development for cancer prevention and therapeutic use. Additionally, our observations also underscore the importance of testing 3HOI-BA-01 in combination with known and conventional chemotherapeutic drugs.

References

1. Guertin DA, Sabatini DM. Defining the role of mTOR in cancer. Cancer Cell. 2007;12:9-22.

2. Hennessy BT, Smith DL, Ram PT, Lu Y, Mills GB. Exploiting the PI3K/AKT pathway for

17

cancer drug discovery. Nat Rev Drug Discov. 2005;4:988-1004.

3.   Manning BD, Cantley LC. AKT/PKB signaling: navigating downstream. Cell.

2007;129:1261-74.

4.   Stephens L, Anderson K, Stokoe D, Erdjument-Bromage H, Painter GF, Holmes AB, et al.

Protein kinase B kinases that mediate phosphatidylinositol 3,4,5-trisphosphate-dependent activation

of protein kinase B. Science. 1998;279:710-4.

5.   Hsu PP, Kang SA, Rameseder J, Zhang Y, Ottina KA, Lim D, et al. The mTOR-regulated

phosphoproteome reveals a mechanism of mTORC1-mediated inhibition of growth factor signaling.

Science. 2011;332:1317-22.

6.   Sarbassov DD, Guertin DA, Ali SM, Sabatini DM. Phosphorylation and regulation of Akt/PKB

by the rictor-mTOR complex. Science. 2005;307:1098-101.

7.   Shaw RJ, Cantley LC. Ras, PI(3)K and mTOR signalling controls tumour cell growth. Nature.

2006;441:424-30.

8.   Faivre S, Kroemer G, Raymond E. Current development of mTOR inhibitors as anticancer

agents. Nat Rev Drug Discov. 2006;5:671-88.

9.   Neshat MS, Mellinghoff IK, Tran C, Stiles B, Thomas G, Petersen R, et al. Enhanced sensitivity

of PTEN-deficient tumors to inhibition of FRAP/mTOR. Proc Natl Acad Sci U S A.

2001;98:10314-9.

10. Choi J, Chen J, Schreiber SL, Clardy J. Structure of the FKBP12-rapamycin complex interacting

with the binding domain of human FRAP. Science. 1996;273:239-42.

11. Yu K, Shi C, Toral-Barza L, Lucas J, Shor B, Kim JE, et al. Beyond rapalog therapy: preclinical

pharmacology and antitumor activity of WYE-125132, an ATP-competitive and specific inhibitor of

18

mTORC1 and mTORC2. Cancer Res. 2010;70:621-31.

12. O'Reilly KE, Rojo F, She QB, Solit D, Mills GB, Smith D, et al. mTOR inhibition induces

upstream receptor tyrosine kinase signaling and activates Akt. Cancer Res. 2006;66:1500-8.

13. Um SH, Frigerio F, Watanabe M, Picard F, Joaquin M, Sticker M, et al. Absence of S6K1

protects against age- and diet-induced obesity while enhancing insulin sensitivity. Nature.

2004;431:200-5.

14. Friesner RA, Banks JL, Murphy RB, Halgren TA, Klicic JJ, Mainz DT, et al. Glide: a new

approach for rapid, accurate docking and scoring. 1. Method and assessment of docking accuracy. J

Med Chem. 2004;47:1739-49.

15. Sherman W, Day T, Jacobson MP, Friesner RA, Farid R. Novel procedure for modeling

ligand/receptor induced fit effects. J Med Chem. 2006;49:534-53.

16. Egle M. Beccalli AMaTP. Synthesis of the carbazole alkaloids hyellazole and 6-chlorohyellazole

and related derivatives J Chem Soc, Perkin Trans 1. 1994:579-87.

17. Xie H, Lin L, Tong L, Jiang Y, Zheng M, Chen Z, et al. AST1306, a novel irreversible inhibitor

of the epidermal growth factor receptor 1 and 2, exhibits antitumor activity both in vitro and in vivo.

PLoS One. 2011;6:e21487.

18. Liu K, Park C, Li S, Lee KW, Liu H, He L, et al. Aloe-emodin suppresses prostate cancer by

targeting the mTOR complex 2. Carcinogenesis. 2012.

19. Berndt A, Miller S, Williams O, Le DD, Houseman BT, Pacold JI, et al. The p110 delta structure:

mechanisms for selectivity and potency of new PI(3)K inhibitors. Nat Chem Biol. 2010;6:117-24.

20. Freedman VH, Shin SI. Cellular tumorigenicity in nude mice: correlation with cell growth in

semi-solid medium. Cell. 1974;3:355-9.

19

21. Gately K, Al-Alao B, Dhillon T, Mauri F, Cuffe S, Seckl M, et al. Overexpression of the mammalian target of rapamycin (mTOR) and angioinvasion are poor prognostic factors in early stage NSCLC: a verification study. Lung Cancer. 2012;75:217-22.

22. Dobashi Y, Suzuki S, Matsubara H, Kimura M, Endo S, Ooi A. Critical and diverse involvement of Akt/mammalian target of rapamycin signaling in human lung carcinomas. Cancer. 2009;115:107-18.

23. McDonald JM, Pelloski CE, Ledoux A, Sun M, Raso G, Komaki R, et al. Elevated phospho-S6 expression is associated with metastasis in adenocarcinoma of the lung. Clin Cancer Res. 2008;14:7832-7.

24. Wanner K, Hipp S, Oelsner M, Ringshausen I, Bogner C, Peschel C, et al. Mammalian target of rapamycin inhibition induces cell cycle arrest in diffuse large B cell lymphoma (DLBCL) cells and sensitises DLBCL cells to rituximab. Br J Haematol. 2006;134:475-84.

25. Cantley LC. The phosphoinositide 3-kinase pathway. Science. 2002;296:1655-7.

26. Markman B, Dienstmann R, Tabernero J. Targeting the PI3K/Akt/mTOR pathway--beyond rapalogs. Oncotarget. 2010;1:530-43.

27. Fruman DA, Meyers RE, Cantley LC. Phosphoinositide kinases. Annu Rev Biochem. 1998;67:481-507.

28. Buck E, Eyzaguirre A, Rosenfeld-Franklin M, Thomson S, Mulvihill M, Barr S, et al. Feedback mechanisms promote cooperativity for small molecule inhibitors of epidermal and insulin-like growth factor receptors. Cancer Res. 2008;68:8322-32.

29. Cloughesy TF, Yoshimoto K, Nghiemphu P, Brown K, Dang J, Zhu S, et al. Antitumor activity of rapamycin in a Phase I trial for patients with recurrent PTEN-deficient glioblastoma. PLoS Med.

20

2008;5:e8.

Figure Legends

Figure 1. Chemical structure of 3HOI-BA-01 and predicted docking mode with mTOR. A, chemical structure of 3HOI-BA-01. B, predicted computational model of the mTOR-3HOI-BA-01 complex. 3HOI-BA-01 is shown in stick model and protein residues are shown in line model. Left panel, the binding pose of 3HOI-BA-01 inside the ATP binding pocket of mTOR. Right panel, the interaction between 3HOI-BA-01 and related residues in the ATP binding pocket.

Figure 2. 3HOI-BA-01 inhibits mTOR kinase activity by directly binding with mTOR. A, 3HOI-BA-01 suppresses mTOR *in vitro* kinase activity in a concentration-dependent manner. An inactive p70S6K protein was used as the substrate for an *in vitro* kinase assay with active mTOR and 100 μM ATP. Proteins were resolved by SDS-PAGE and detected by Western blotting. B and C, 3HOI-BA-01 binds directly to mTOR *in vitro* (B) and *ex vivo* (C). Sepharose 6B beads were used for binding and pull-down assays as described in Materials and Methods. Lane 1 is input control (mTOR protein standard); lane 2 is the negative control, indicating no binding between mTOR and Sepharose 6B beads; and lane 3 shows that mTOR binds with 3HOI-BA-01-Sepharose 6B beads.

Figure 3. 3HOI-BA-01 inhibits EGF-induced neoplastic transformation and signal transduction in JB6 Cl41 cells. A, 3HOI-BA-01 inhibits EGF-induced anchorage-independent growth of JB6 Cl41 cells. B, quantification data for panel A. The asterisk (*) indicates a significant ($p < 0.01$) decrease in colony formation in cells treated with 3HOI-BA-01 compared with the DMSO-treated group. C,

21

cytotoxic effects of 3HOI-BA-01 on JB6 Cl41 cells. An MTS assay was used after treatment of cells

with 3HOI-BA-01 for 24 or 48 h, respectively. D, 3HOI-BA-01 inhibits mTOR downstream signal

transduction in JB6 Cl41 cells. After starvation in serum-free medium for 24 h, cells were treated

with 3HOI-BA-01 at the indicated concentrations for 2 h and then stimulated with EGF (20 ng/mL)

for 15 min. Cells were then harvested and protein levels were determined by Western blot analysis.

Figure 4. Effects of 3HOI-BA-01 on anchorage-independent growth and mTOR signaling in lung

cancer cells. A to C, 3HOI-BA-01 inhibits anchorage-independent growth in a panel of NSCLC cell

lines, including A549 cells (A), H520 cells (B) and H1650 cells (C). The asterisk (*) indicates a

significant ($p < 0.01$) decrease in colony formation in cells treated with 3HOI-BA-01 compared with

the DMSO-treated group. D, 3HOI-BA-01 inhibits mTOR signaling in A549 cells. Cells were

starved in serum-free medium for 24 h, and then treated with 3HOI-BA-01 at the indicated

concentrations for 2 h. After stimulation with EGF (20 ng/mL) for 15 min, cells were harvested and

protein levels were determined by Western blot analysis. E, 3HOI-BA-01 treatment results in G1 cell

cycle arrest. Cell cycle analysis was performed on A549 cells treated or not treated with

3HOI-BA-01 (10 µM) for 72 h. Cell cycle distribution is labeled on the histogram.

Figure 5. Effects of 3HOI-BA-01 on PI3-K and Akt *in vitro* kinase activity. A, at a high

concentration, 3HOI-BA-01 inhibits PI3-K α, β and δ activities. B, 3HOI-BA-01 exerts a weak

inhibition on Akt1 and Akt2 kinase activity. The kinase assays are described in detail in Materials

and Methods.

22

Figure 6. Effect of 3HOI-BA-01 on lung cancer growth and mTOR targets in an A549 xenograft mouse model. A, 3HOI-BA-01 significantly suppresses lung cancer cell growth. The average tumor volume of vehicle-treated control mice and 3HOI-BA-01-treated mice plotted over 29 days after tumor cell injection. The *P* values indicate a significant inhibition by 3HOI-BA-01 on tumor growth (*, $p < 0.05$; **, $p < 0.01$). B, 3HOI-BA-01 has no effect on mouse body weight. Body weights from treated or untreated groups of mice were measured once a week. C, 3HOI-BA-01 inhibits mTOR-targeted protein expression in A549 lung cancer tissues. The tumor tissues from groups treated with vehicle or 10 mg 3HOI-BA-01/kg body weight were immunoblotted with antibodies to detect the expression of total- and phospho-S6 and Akt proteins. Expression of β-actin was used to verify equal protein loading.

23

Figure 1 A-B

A

B

Figure 2 A-C

A

p-p70S6K (T389)
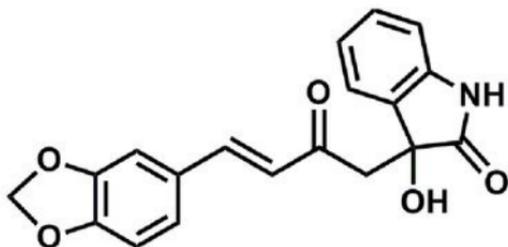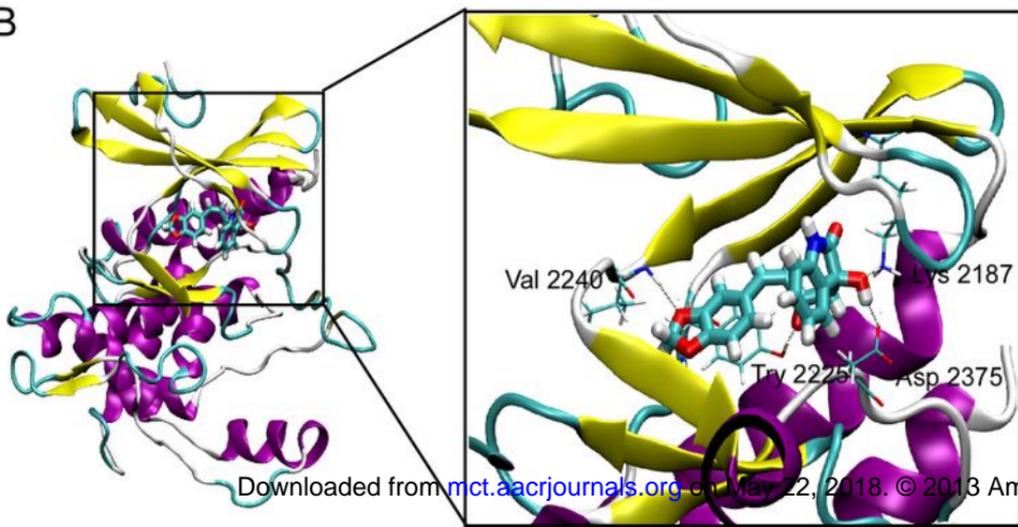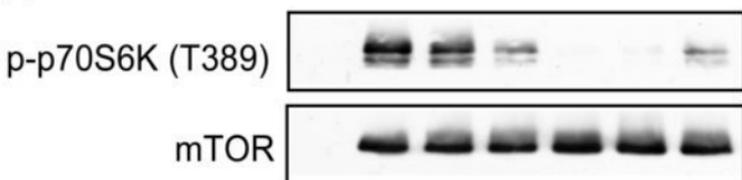
mTOR

active mTOR	-	+	+	+	+	+	+
inactive p70S6K	+	+	+	+	+	+	+
3HOI-BA-01 (μM)	-	-	1	5	10	20	-
Wortmannin (μM)	-	-	-	-	-	-	2
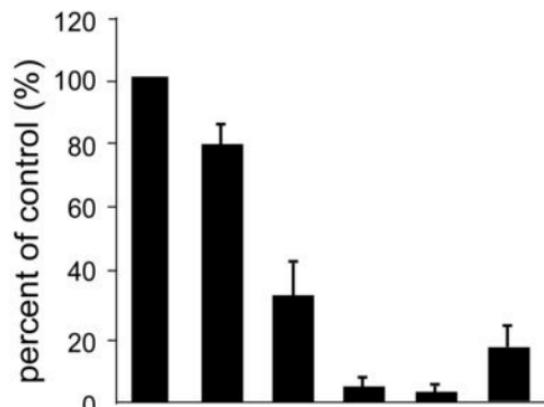
3HOI-BA-01 (μM)   -   1   5   10   20   -
Wortmannin (μM)   -   -   -   -   -   2

B
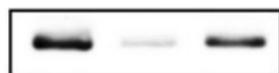
active mTOR	+	+	+
epoxy-Sepharose 6B	-	+	-
3HOI-BA-01 Sepharose 6B	-	-	+

C
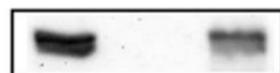
cell lysate	+	+	+
epoxy-Sepharose 6B	-	+	-
3HOI-BA-01 Sepharose 6B	-	-	+

Figure 3 A-D

Figure 4 A-E

A A549

B H520

C H1650
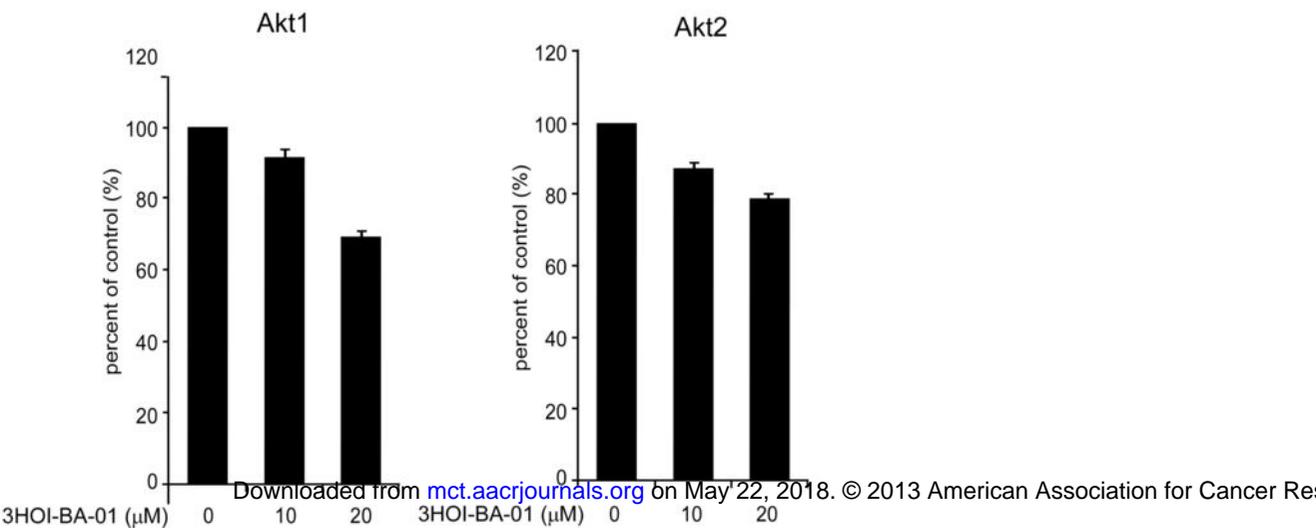
D

E

Figure 5 A-B

Figure 6 A-C
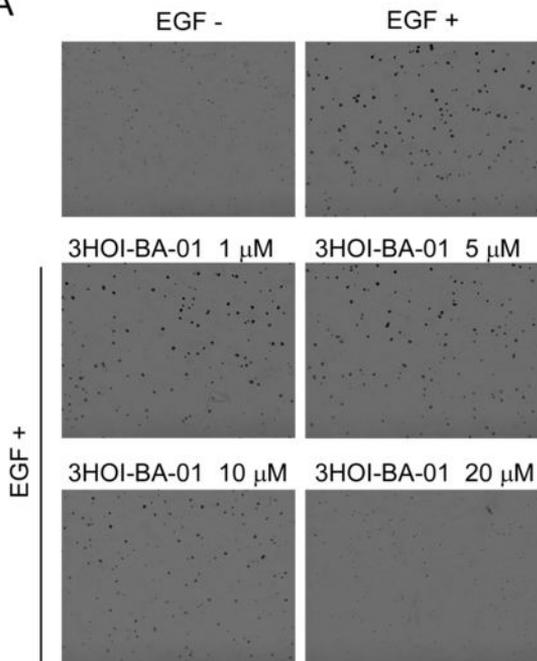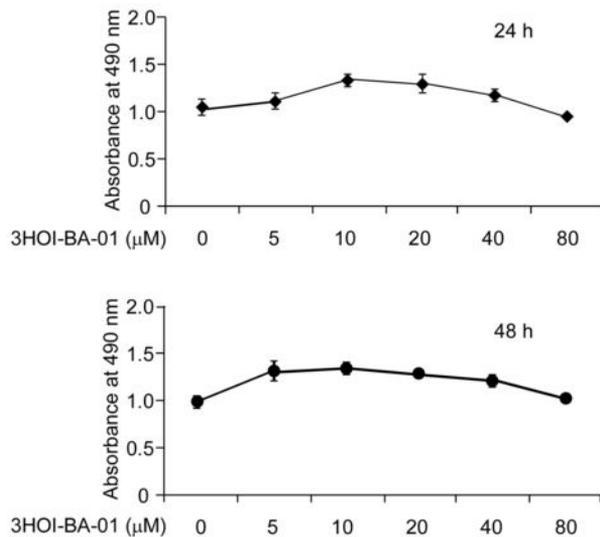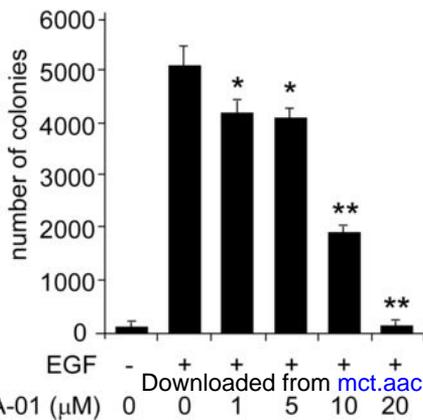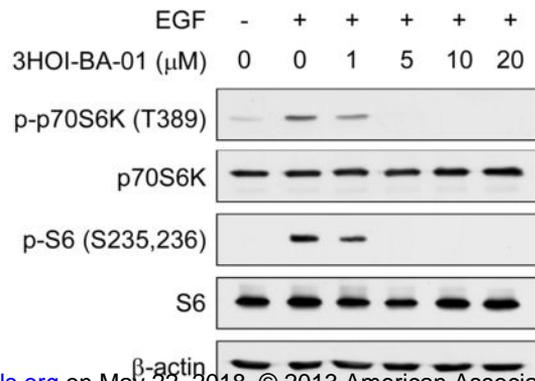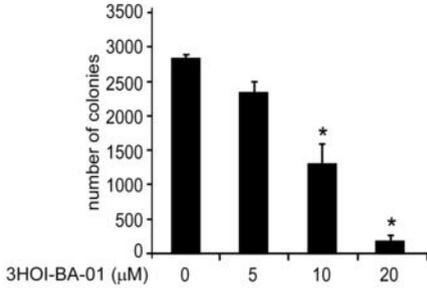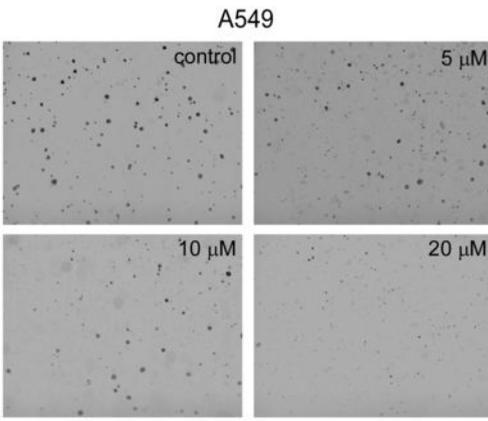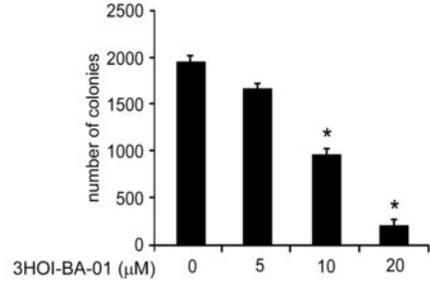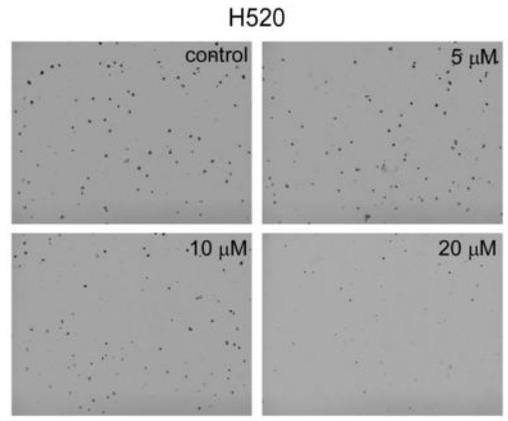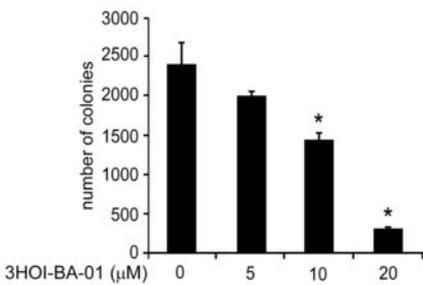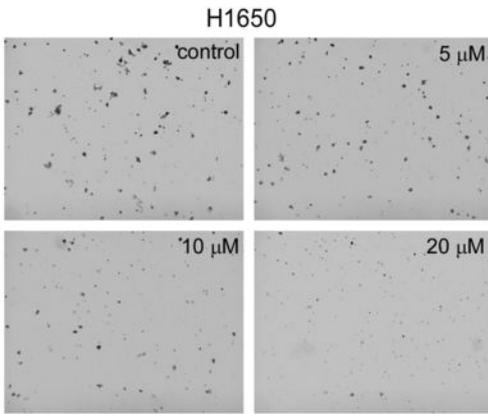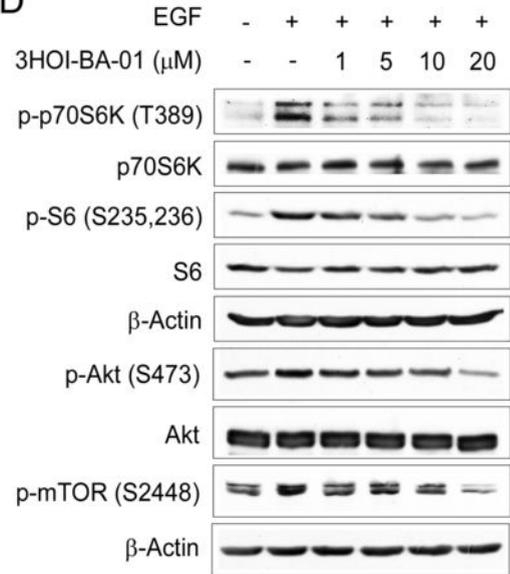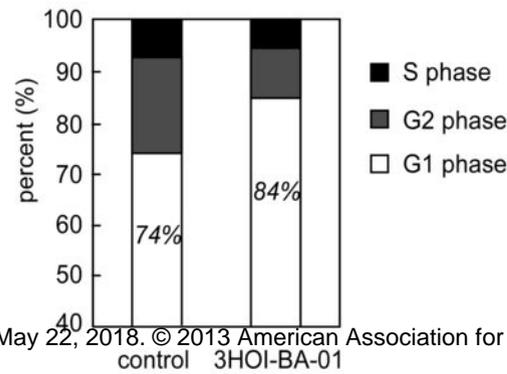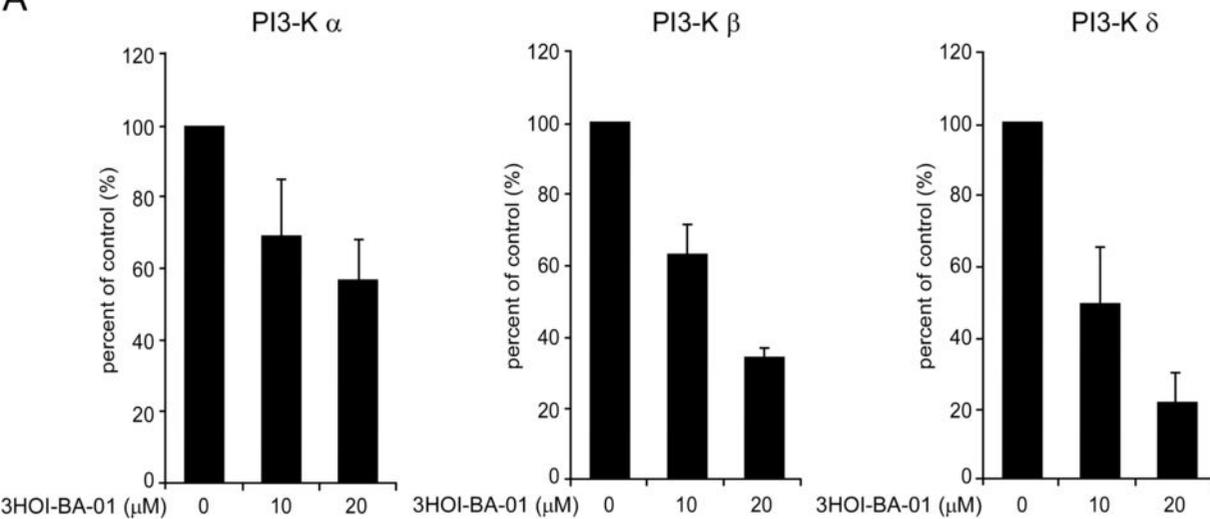
A

B

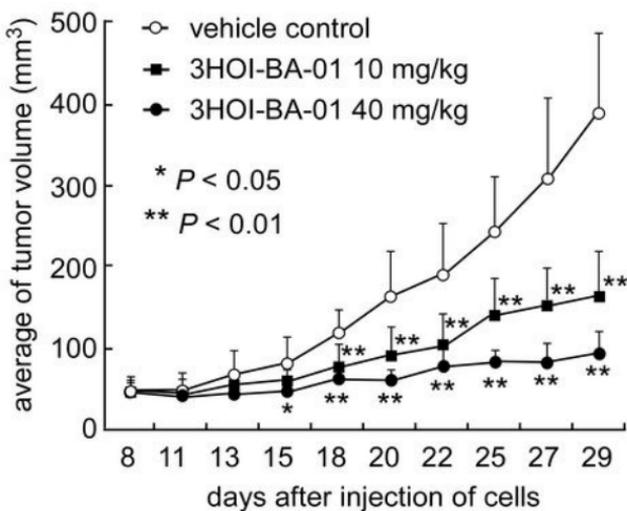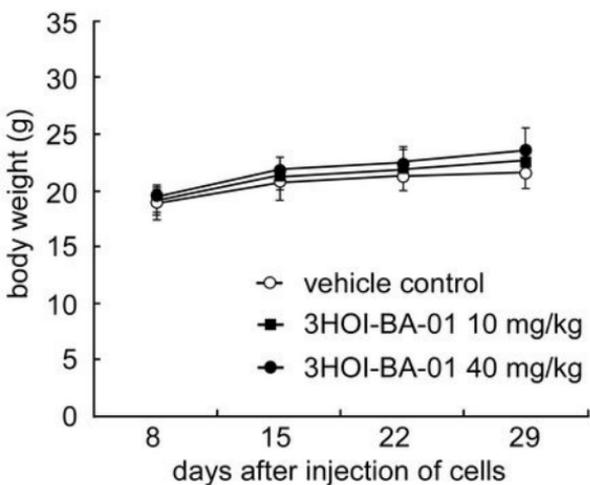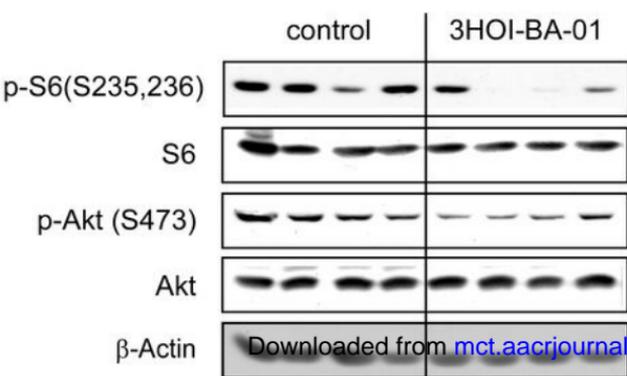## C

Molecular Cancer Therapeutics

Discovery of the novel mTOR inhibitor and its antitumor activities in vitro and in vivo

Hua Xie, Mee-Hyun Lee, Feng Zhu, et al.

Updated version	Access the most recent version of this article at: doi:10.1158/1535-7163.MCT-12-1241
Author Manuscript	Author manuscripts have been peer reviewed and accepted for publication but have not yet been edited.

E-mail alerts	Sign up to receive free email-alerts related to this article or journal.
Reprints and Subscriptions	To order reprints of this article or to subscribe to the journal, contact the AACR Publications Department at pubs@aacr.org.
Permissions	To request permission to re-use all or part of this article, use this link http://mct.aacrjournals.org/content/early/2013/03/21/1535-7163.MCT-12-1241. Click on "Request Permissions" which will take you to the Copyright Clearance Center's (CCC) Rightslink site.